JOURNAL OF MATERIALS SCIENCE 33 (1998) 2919–2925

Material properties of $CuInSe_2$ prepared by H_2Se treatment of CuIn alloys

V. ALBERTS, R. SWANEPOEL
Department of Physics, Rand Afrikaans University, PO Box 524, Auckland Park 2006, South Africa
E-mail: VA@na.rau.ac.zd.

M. J. WITCOMB
Electron Microscope Unit, University of the Witwatersrand, Bag 3, WITS 2050, South Africa

$CuInSe_2$ thin films were prepared by the selenization of metallic precursors in an atmosphere containing H_2Se gas. Device-quality (homogeneous and dense films with excellent compositional uniformity) $CuInSe_2$ films were obtained when Cu/In/Cu structures were exposed to H_2Se/Ar while the temperature was ramped between 150 and 400 °C. Auger studies indicated that the composition of the films was relatively uniform through their thickness. Transmission electron microscopy studies indicated that copper-rich samples exhibited large facetted grains (1–4 μm) with relatively low defect density. Indium-rich films were characterized by relatively small grains (0.2–0.8 μm), which were highly defected. $CuInSe_2$/CdS/ZnO solar cells were fabricated using chemically etched (in KCN) copper-rich $CuInSe_2$ absorber films, and conversion efficiencies of 5% were obtained without the use of an antireflection coating. © *1998 Kluwer Academic Publishers*

1. Introduction

$CuInSe_2$ and related compound semiconductors containing gallium and sulphur are important photovoltaic materials with electrical and optical properties that can be tuned for optimum device performance. Thin-film solar cells with active area efficiencies in the range of 17% have already been fabricated on such absorber layers [1]. Even more important, these devices have shown virtually no evidence of degradation with time. The $CuInSe_2$ thin-film processing approaches currently in use can be grouped under two main categories; single-stage processing approaches and two-stage processing approaches. In general, two-stage processing methods for $CuInSe_2$ are relatively easy scalable techniques which can produce a uniform coating of thin films on large area substrates. Selenization (in selenium vapour or an H_2Se/Ar atmosphere) of vacuum-processed CuIn alloys is one of the most promising two-stage approaches in use today. Using this technique, Basol *et al.* [2] recently demonstrated small-area solar cells with efficiencies above 12%, which is only slightly behind the best results of co-evaporated $CuInSe_2$ solar cells. These workers also demonstrated $CuInSe_2$/CdS/ZnO modules with efficiencies above 7%, clearly demonstrating that this process can be scaled up for mass production [3].

Deposition of $CuInSe_2$ absorber layers with controlled stoichiometry, compositional uniformity and good surface morphology, is the heart of this technology. In this study, $CuInSe_2$ thin films were prepared by the selenization of metallic elemental layers in an atmosphere containing H_2Se. Attention was mainly focused on the optimization of various growth parameters for the production of device-quality $CuInSe_2$ absorber layers. The material properties (structural, optical and electrical) of the semiconductor thin films were subsequently evaluated and are discussed in this paper. The device characteristics of preliminary $CuInSe_2$/CdS/ZnO solar cells are also discussed.

2. Experimental procedure

2.1. Film deposition

The $CuInSe_2$ films studied in the present work were deposited on 5×5 cm^2 soda–lime glass substrates. In the first step of the process, thin layers of molybdenum, copper and indium were deposited on the glass substrates using electron-beam evaporation. A single, rotatable, crucible permitted the sequential deposition of molybdenum, copper and indium in any desired order and thickness without breaking the vacuum. The thicknesses of the copper and indium layers were typically 0.2–0.25 and 0.4–0.45 μm, respectively, in order to vary the Cu/In atomic ratio between 0.8 and 1.2. The thicknesses of the molybdenum, copper and indium layers were measured by a quartz crystal thickness monitor and confirmed by DEKTAK measurements. Deposition was carried out at a pressure of about 5×10^{-6} torr (1 torr = 133.322 Pa) at

0022–2461 © *1998 Kluwer Academic Publishers*

a deposition rate of 0.1 nm s^{-1}. A series of samples was prepared in order to optimize the copper and indium deposition parameters [4]. The thicknesses of all the different structures were such that the selenized films obtained were approximately 2 μm thick. The grown structures were subsequently annealed (120 °C for 3 h) under vacuum to ensure complete mixing of copper and indium by diffusion. After the evaporation, the substrates were removed from the vacuum and placed in a diffusion furnace in which they were exposed to a mixture of H_2Se and argon gases (10%–15% H_2Se in argon) at atmospheric pressure. A standard diffusion furnace as routinely used in the integrated circuit (IC) technology was employed in this study. The selenization temperature profile and exposure period were varied to optimize conditions so that films of good mechanical properties could be obtained. Prior to cell fabrication, copper-rich samples were etched in a 5% KCN solution at room temperature. After chemical treatment, the absorber layers were immediately covered with a thin (20–30 nm) CdS buffer layer deposited by a wet chemical dip process. Devices were completed with the deposition of a r.f.-sputtered ZnO/ZnO:Al window layer. Ohmic contacts to the ZnO window layer were obtained by the evaporation of Ni/Al through a metal mask.

2.2. Characterization

The surface morphologies of the $CuInSe_2$ thin films were studied by scanning electron microscopy (SEM), and the bulk composition was determined with energy dispersive X-ray spectroscopy (EDS). The compositional uniformities of the grown $CuInSe_2$ samples were investigated by Auger electron spectroscopy (AES). Depth profiling was carried out with Ar^+ sputtering at 3 kV accelerating voltage and 25 mA emission current. The crystalline phases present were examined by X-ray diffraction (XRD) and the crystallinity and defect structure of the $CuInSe_2$ samples were evaluated in a Philips CM20 microscope operating at 200 kV. Transmission electron microscopy (TEM) samples were prepared by mechanically polishing the samples down to 20 μm thickness, followed by ion milling using 5 kV Ar ions at a 15° incidence angle. Excessive sample heating and damage during ion milling were minimized by using a liquid nitrogen-cooled specimen stage. The resistivity of the samples was measured by the four-point probe method, while the conductivity type was determined by the hot probe test. Carrier concentrations were determined by Hall and capacitance–voltage (C–V) measurements. Photoluminescence (PL) measurements were carried out using a 40 mW krypton-ion-laser at an excitation wavelength of 568.2 nm. Solar cells were evaluated by standard I–V and quantum efficiency measurements.

3. Results

The optimization of the structural (surface morphology, adhesion and compositional uniformity), optical and electrical properties of the $CuInSe_2$ absorber layer is an important prerequisite for the successful fabrication of highly efficient $CuInSe_2$/CdS/ZnO solar cells. In this study, attention was mainly focused on the characterization of copper-rich $CuInSe_2$ samples which were used for solar cell applications.

3.1. Structural properties of $CuInSe_2$

We have demonstrated in a previous study [4] that the structural properties (morphology and compositional uniformity) of the resulting compound film depend strongly on how the elemental layers (copper and indium) are deposited on the molybdenum-coated glass substrates. The degree of alloy formation (determined by the deposition parameters) and the sequence of evaporation of the precursor elements are some of the important factors which strongly influence the quality of the $CuInSe_2$ films obtained. SEM studies indicated, for example, that Cu/In bilayers (without any intentional heating) were characterized by rough and discontinuous surface morphologies. In the case where these structures were evaporated on to heated substrates, large facetted grains superimposed to a thin, uniform layer were observed (droplet structure).

Deposition of copper layers over indium layers (In/Cu bilayers) resulted in alloys which were characterized by a high density of small grains. Selenization of these bilayer structures (i.e. Cu/In and In/Cu) generally resulted in compound films with poor structural properties (rough and non-uniform surface morphologies) and associated large variations in the composition. In the case of Cu/In/Cu triple layers, alloys with smooth surface morphologies (absence of droplets on the surface) and good adhesion properties were obtained. Selenization of such optimized precursors resulted in $CuInSe_2$ films with relatively uniform and dense surface morphologies and a high degree of compositional uniformity.

While CuIn alloys of good morphology are required in order to obtain high-quality $CuInSe_2$ films, the selenization step appeared to be no less critical. In the case of CuIn precursor films (bilayers, triple layers and multilayers) exposed directly to H_2Se at 400 °C (30–60 min), films with poor structural properties were obtained [5]. These films were characterized by the presence of morphological boundaries and poor adhesion properties. The poor structural properties of the $CuInSe_2$ films, selenized directly at high temperature, is explained by the rapid and uncontrolled incorporation of selenium into the CuIn films during this process.

A drastic improvement in the structural properties (adhesion properties and morphology) of the compound films were observed when the CuIn films were exposed to H_2Se while ramping the temperature. Optimum material properties were obtained when Cu/In/Cu triple layers were exposed to H_2Se/Ar while ramping the temperature between 150 and 400 °C.

To the naked eye, stoichiometric or copper-rich samples appeared compact and uniform, whereas indium-rich films were characterized by a more irregular structure. Fig. 1a and b are representative planar- and cross-sectional view scanning electron

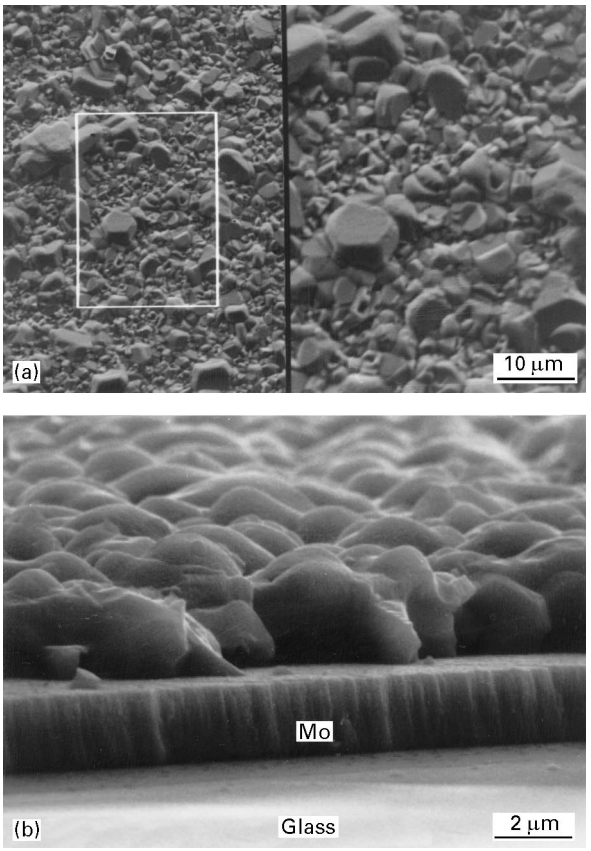

Figure 1 (a) Planar- and (b) cross-sectional view scanning electron micrographs of a typical copper-rich $CuInSe_2$ film (28.6 at % Cu, 22.3 at % In and 49.1 at % Se) prepared in this study. The samples were prepared by the selenization (in H_2Se/Ar while ramping the temperature) of Cu/In/Cu metallic alloys.

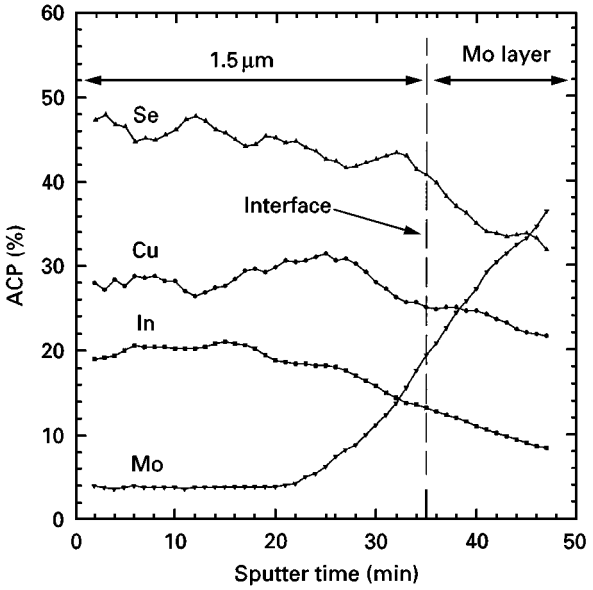

Figure 2 Auger depth profile of the $CuInSe_2$ sample shown in Fig. 1.

micrographs of a typical copper-rich sample prepared in this study. Although large crystals with clear {1 1 1} facets were present, the majority of the crystals were of relatively constant size for a given Cu/In atomic ratio (see Fig. 1a). Careful spot-mode X-ray micro-analysis indicated that the smaller grained matrix consisted of slightly copper-rich chalcopyrite grains while the large grains were almost completely depleted of indium [4]. The large smooth-faced crystallites of Cu_2Se on the surface of copper-rich samples were also observed by other workers [6] and are attributed to the high mobility of copper species during the reaction step (in H_2Se/Ar) which gives rise to the total separation of Cu_2Se grains throughout the selenized films. This phenomenon therefore implies that the selenization of copper-rich precursors yielded a $CuInSe_2 + Cu_2Se$ layer with segregated Cu_2Se grains. The superior adhesion properties of the selenized (in H_2Se/Ar atmosphere) copper-rich precursors are clearly evident in Fig. 1b.

The determination of the compositional properties with depth is an important consideration for electronic materials and device fabrication. The EDS results (at 25 kV), given in Fig. 1, represent average values from 40 different locations on the film. Under these experimental conditions, and assuming compositional uniformity with depth, the normalized atomic per cent values may be considered to represent bulk values. The samples were subsequently investigated by Auger electron microscopy in order to obtain an accurate evaluation of the compositional uniformity with depth. Fig. 2 represents the Auger data taken from the $CuInSe_2$ layer shown in Fig. 1b. The total thickness of this specific film was about 1.5 μm. The analysis was done at different locations on the film, the result illustrated in Fig. 2 being typical of one of these spot analyses. It can be seen from this profile that the composition of the film is relatively uniform through its thickness and that the measured values are in good agreement with the measured EDS results. It is also important to note that the AES depth compositional profile indicates a significant inter-diffusion between the molybdenum back contact layer and the $CuInSe_2$ film. This phenomenon has also been observed by other workers [7]. It is believed that any pinholes present in the molybdenum layer could permit a certain degree of interaction between the $CuInSe_2$ film and the underlying molybdenum layer. In extreme cases of a high degree of interaction between molybdenum and especially selenium, adhesion problems were detected.

The crystalline quality of the prepared films were evaluated by X-ray diffraction (XRD) measurements. Fig. 3a is an XRD pattern of the copper-rich sample, shown in Fig. 1. In addition to the typically expected reflections of the chalcopyrite structure, a few extra lines of weak intensity are visible. Careful analysis revealed that these additional peaks are related to the presence of $Cu_{2-x}Se$ (JCPDS: 6-680) and Cu_2Se (JCPDS: 27-1131). The presence of low-resistivity phases such as $Cu_{2-x}Se$ and Cu_2Se in appreciable quantities in $CuInSe_2$ layers would prevent high-efficiency solar cells being fabricated. However, these binary copper-chalcopyrite secondary phases were easily removed by etching in the copper-rich samples in a KCN solution. After chemical treatment, EDS analysis indicated a slight excess of In (23.5 at % Cu, 25.6 at % In and 50.9 at % Se) in the bulk. Fig. 3b shows an XRD pattern for a typical chemically treated

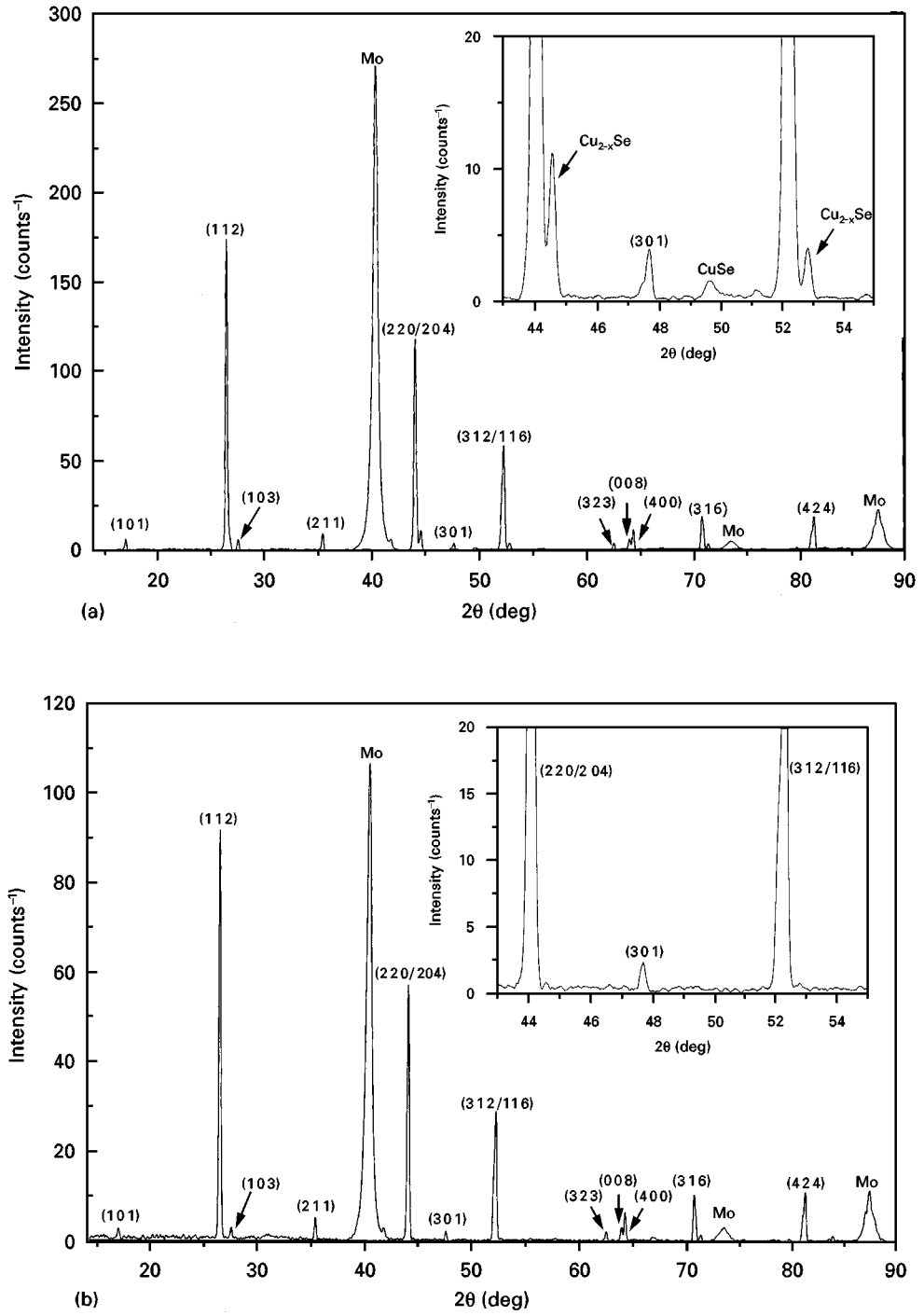

Figure 3 X-ray diffraction patterns obtained from (a) copper-rich and (b) KCN-treated $CuInSe_2$ samples.

sample. This pattern is in good agreement with the reported features of stoichiometric samples, showing only the allowed reflections of the chalcopyrite structure. The lattice constants measured for the etched copper-rich samples were $a = 0.5786 \pm 0.0001$ nm and $c = 1.1614 \pm 0.0004$ nm ($c/a = 2.007$), which is in good agreement with published single-crystal data [8].

The grain structure of $CuInSe_2$ absorber layers in solar cells is critically related to the performance of the resulting device. It was generally observed in this study that stoichiometric or copper-rich samples were compact and uniform, whereas indium-rich samples exhibited smaller grains and a more irregular structure. The resulting microstructure of copper- and indium-rich $CuInSe_2$ films (prepared by selenization of CuIn alloys) were analysed in more detail by transmission electron microscopy (TEM). Fig. 4a is a representative bright-field planar view TEM image of the copper-rich film shown in Fig. 1. The sizes of grains in the copper-rich films were found to be relatively large, ranging from 1–4 μm diameter, although grains as small as 0.1 μm were also observed. The grain boundaries (indicated by G) are clearly visible between the individual grains (see Fig. 4a). The lattice defects in Fig. 4a were analysed using bright- and dark-field imaging. This analysis revealed that copper-rich films are characterized by fairly low defect densities. The only defects present in these samples with significant

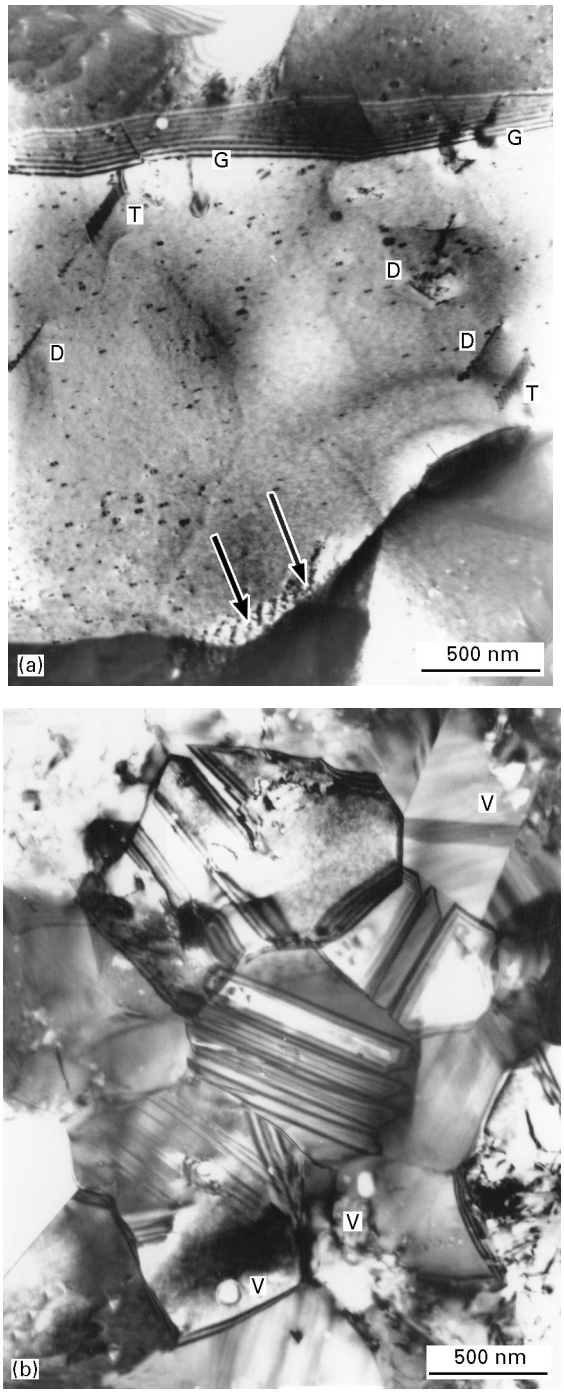

Figure 4 Bright-field planar view transmission electron micrographs of (a) copper-rich and (b) indium-rich samples, prepared by the selenization of metallic precursors.

density were dislocations (indicated by D). Although these defects were frequently observed, there was no evidence of major dislocation tangles. The high atomic mobility, as is evident by the formation of $CuInSe_2$ by selenization of copper and indium layers at 400 °C for 60 min, may assist climb mechanisms, permitting the escape of dislocations. Small dislocation loops, exhibiting characteristic black-lobe contrast, are also clearly visible in Fig. 4a. Another interesting feature of the copper-rich samples is the presence of fine precipitates (indicated by arrows) in the close vicinity of some of the grain boundaries. Microtwins and/or stacking faults (indicated by T) were occasionally observed in the copper-rich grains.

In contrast to copper-rich films, dislocations and dislocation loops could not be detected in indium-rich $CuInSe_2$ films. These films (see Fig. 4b) exhibited much smaller (0.2–0.8 μm), facetted grains which were highly defected. The most common defects present were planar defects in the form of microtwins and/or stacking faults which usually extended across the whole grain width. These defects probably occur due to "growth accidents" on the advancing close packed $\{1\,1\,2\}$ type planes because the bond distortion associated with the occupation of incorrect sites on this plane is quite small [9]. A significant number of voids (indicated by V) were also detected in our standard indium-rich material. While these voids did not constitute a significant percentage of the volume of the film, it may be necessary to eliminate them in order to achieve the highest solar conversion efficiency.

3.2. Optical and electrical properties of $CuInSe_2$

When preparing samples for optical and electrical measurements, the molybdenum layers were normally omitted. As expected, the resistivities of $CuInSe_2$ films (measured by the four-point probe method) were found to be strongly dependent on their bulk composition (determined by EDS). Copper-rich films (Cu/In atomic ratio = 1.1–1.3) were found to be p-type having resistivities in the 10^{-2}–$10^{-1}\,\Omega\,cm$ range at room temperature. The low resistivity values measured for copper-rich samples ($N_A \simeq 10^{18}$–$10^{19}\,cm^{-3}$) can be attributed to the presence of intergranular Cu_2Se precipitates which exhibit quasi-metallic conduction. Indium-rich films (Cu/In atomic ratio = 0.9–0.6) of comparable thickness were characterized by fairly high resistivities ($\rho = 10^1$–$10^3\,\Omega\,cm$). However, it is important to mention that these resistivity values were very sensitive to annealing in argon and H_2Se. Annealing of the films in argon improved the n-type electrical properties, while an H_2Se anneal promoted p-type conductivity. It was, for example, observed that the resistivity values of copper-rich material could be increased by a few orders of magnitude by annealing the layers in argon for a few hours. Capacitance–voltage measurements (not shown) were used to obtain depth profiles of the majority carrier concentration in chemically treated (5% KCN) $CuInSe_2$ samples. These measurements (as a function of temperature) indicated that the device capacitance was critically influenced by contributions of gap-states in the depletion region to the capacitance. The doping profiles (not shown), deduced from the Mott–Schottky plots, indicated carrier densities in the range 2–$5 \times 10^{16}\,cm^{-3}$ (80–300 K) for KCN etched copper-rich samples. However, due to the deep state contributions, the interpretation of the C–V data is not straightforward. These results will be discussed in more detail in a forthcoming article.

Figure 5 shows the photoluminescence spectra for a typical copper-rich sample at different temperatures (6–80 K). At low temperatures (6 K), four well-defined emission lines and one shoulder (indicated by arrow)

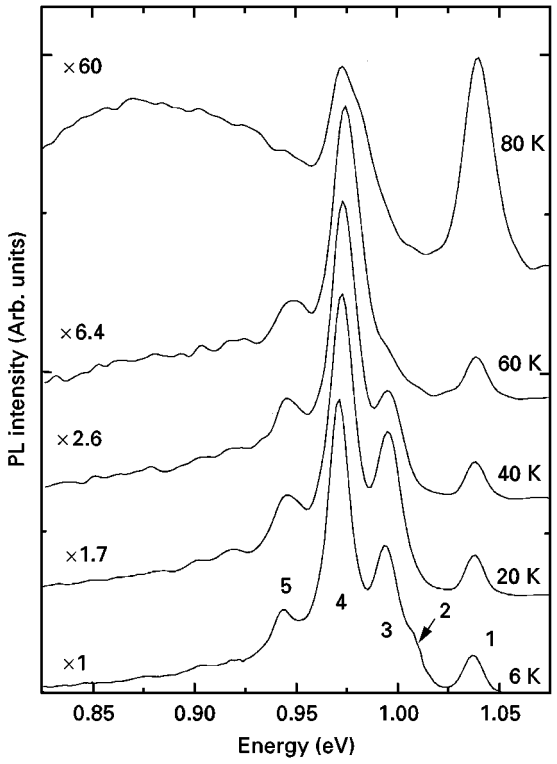

Figure 5 General features of a photoluminescence spectrum (6–80 K) obtained from a copper-rich polycrystalline $CuInSe_2$ sample.

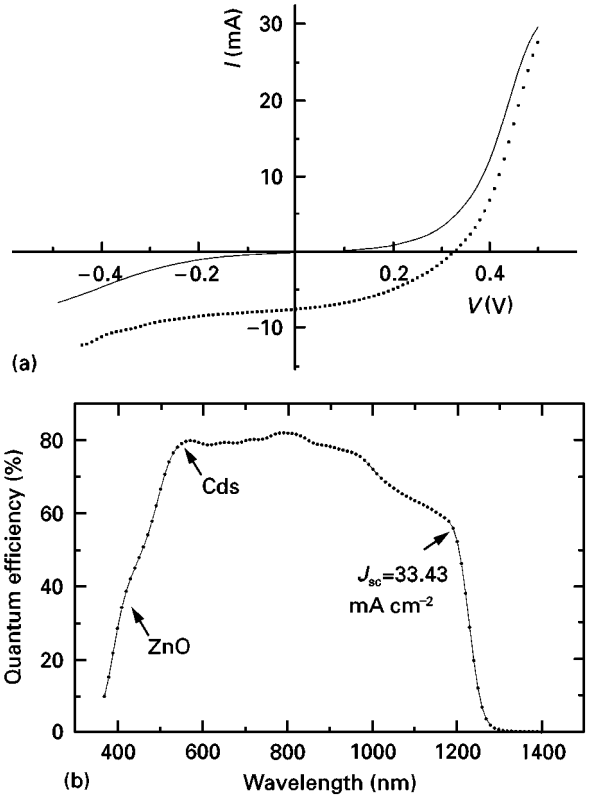

Figure 6 Comparison of the (a) *I–V* characteristics, and (b) quantum efficiency for a $CuInSe_2$/CdS/ZnO solar cell where a KCN-etched $CuInSe_2$ absorber film was used. (a) $V_{oc} = 354.4$ mV, $I_{sc} = -8.35$ mA, FF = 0.42, $A = 0.25\ cm^{-2}$, $\eta = 5\%$.

are visible. The photoluminescence properties of these copper-rich samples are in good agreement with the PL emissions observed from single-crystalline MBE grown $CuInSe_2$ [10]. The near band-edge emission, peak 1 (1.036 eV), could be ascribed to an exciton-related emission. The energy separation of 28 meV between peak 1 and the shoulder 2 at 1.008 eV is comparable with the reported value for the longitudinal optical (LO) phonon energy in $CuInSe_2$ [11]. Intensity-dependent measurements indicated no shift of peaks 3 (0.993 eV) and 4 (0.971 eV). These transitions are, therefore, considered to be bound to free transitions. The remaining peak 5 at 0.942 eV has also been identified as an LO phonon replica of peak 4. It is interesting to note from Fig. 5 that, at temperatures above 60 K, a broad peak at 0.90 eV becomes dominant. From excitation power-dependent measurements (not shown), the radiative recombination process of this emission line is considered to be a donor–acceptor pair transition. A detailed discussion of the optical properties of $CuInSe_2$, as a function of composition, is presented elsewhere [12].

3.3. Device properties

Preliminary $CuInSe_2$/CdS/ZnO heterojunction solar cells were fabricated using a standard technology (chemical bath deposition CdS, r.f.-sputtered ZnO and Ni/Al contacts). These solar cell devices were fabricated on copper-rich (etched in KCN) absorbers which were characterized by superior structural properties (large grains with relatively low defect density). Fig. 6a shows the *I–V* characteristics of such a cell, evaluated under simulated AM 1.5 (100 mW cm^{-2}) conditions at 25 °C. The total area of the device is 0.25 cm^2. With an open-circuit voltage, $V_{oc} = 354.4$ mV, a short-circuit current density, $J_{sc} = 33.4\ mA\ cm^{-2}$, and a fill factor of 42%, such a cell has a solar conversion efficiency typically of 5%. The performances of these devices were mainly limited by high reverse dark currents (see Fig. 6a). This phenomenon, limiting the open-circuit voltage and fill factor of the device, is attributed to shunting paths created in the material after cyanide treatment. It is therefore important to realize that the total separation of Cu_2Se grains throughout the selenized film (see Fig. 1a) presents a serious problem for device applications. The formation of the Cu_2Se nodules is directly linked to the specific growth conditions of our fabrication process and cannot be eliminated by simply reacting the film with additional indium. The present approach of removing these copper-rich grains (with associated low resistivities) by chemical etching creates shunt paths in the material and so limits the performance of the device. However, further experiments are in progress to optimize growth conditions (especially selenization parameters) in order to obtain absorbers with optimal composition. Fig. 6b shows the typical photoresponse of a cell fabricated on chemically treated copper-rich material. The cut-offs at short wavelengths (< 500 nm) are due to absorption in the CdS and ZnO layers, while the long-wavelength cut-off corresponds fairly well with the absorption edge

(1.04 eV) of a $CuInSe_2$ thin film. A maximum quantum yield of 82.7% is obtained at $\lambda = 760$ nm. The overall response is relatively flat, indicating a sufficiently large collection width (i.e. space charge region plus diffusion length). However, some losses for the long wavelengths (900–1200 nm) were normally observed in the case of these specific cells. These red losses could explain the non-maximal values obtained for the obtained photocurrent densities.

4. Conclusion

The present results demonstrate the feasibility of obtaining device-quality $CuInSe_2$ absorber layers by the selenization (in H_2Se/Ar) of metallic precursors. The focus of the present work was mainly on the growth and characterization of copper-rich $CuInSe_2$ absorber films. Device-quality absorber layers were prepared when Cu/In/Cu precursors were selenized in H_2Se/Ar while ramping the temperature. The electrical properties of these layers were controlled accurately by small changes in the composition and additional annealing in argon or H_2Se. TEM studies indicated that copper-rich samples are, in general, characterized by the presence of fairly large (1–4 μm), relatively defect-free grains. The only defects present in these samples with significant density are dislocations and dislocation loops. The optical properties (studied by photoluminescence) of the polycrystalline copper-rich films are in good agreement with the reported data for single-crystalline MBE-grown $CuInSe_2$. Preliminary solar cells were fabricated, using these copper-rich absorber films. However, the performances of these devices were mainly limited by relatively low open-circuit voltages and fill factors, which is attributed to shunting paths created in the material after KCN etching. The use of absorbers with optimal composition is expected to yield devices with efficiencies exceeding 10%.

Acknowledgements

The authors acknowledge the technical assistance of Mr E. Scholtz. The assistance of W. Louw (CSIR) with Auger measurements and J. H. Schön, University of Konstanz, with PL measurements is gratefully appreciated. *IV* and quantum efficiency measurements were conducted at IPE in Stuttgart. The financial support of the FRD and the University of the Witwatersrand via the Microstructural Studies Research Programme is also acknowledged.

References

1. J. HEDSTRÖM, H. OHLSÉN, M. BODEGARD, A. KYLNVER, L. STOLT, D. HARISKOS, M. RUCKH and H. W. SCHOCK, in "Proceedings of the 23rd IEEE PVSC" (IEEE, New York, 1993) p. 364.
2. B. M. BASOL, V. K. KAPUR and A. HALANI, in "Proceedings of the 22nd IEEE PVSC" (IEEE, New York, 1991) p. 893.
3. V. K. KAPUR, B. M. BASOL and E. S. TSENG, *Solar Cells* **21** (1987) 65.
4. V. ALBERTS and R. SWANEPOEL, *J. Mater. Sci. Mater. Electron.* **7** (1996) 91.
5. *Idem*, in "Proceedings of the 13th IC PVSEC" (edited by H. S. Stephens, Bedford, 1995) p. 1933.
6. C. D. LOCKHANDE and G. HODES, *Solar Cells* **21** (1987) 215.
7. B. M. BASOL, V. K. KAPUR, A. HALANI, A. MINNICK and C. LEIDHOLM, in "Proceedings of the 23rd IEEE PVSC" (IEEE, New York, 1993) p. 426.
8. J. BINSMA, L. J. GILING and J. BLOEM, *J. Crystal Growth* **50** (1980) 429.
9. F. ERNST and P. PIROUIZ, *J. Appl. Phys.* **64** (9) (1988) 90.
10. S. NIKI, Y. MAKITA, A. YAMADA, A. OBARA, S. MISAWA, O. IGURASHI, K. OAKI and N. KUTSUDAWA, *Jpn J. Appl. Phys.* **33** (1994) L500.
11. H. TANINO, T. MAEDA, H. FUJUKAKE, H. NAKANISHI, S. ENDO and T. IRIE, *Phys. Rev.* **B45** (1992) 13323.
12. J. H. SCHÖN, V. ALBERTS and E. BUCHER, *Thin Solid Films* **301** (1997) 115.

Received 23 October 1996
and accepted 3 March 1998